

# Characterization of Electrochromic Vanadium Pentoxide Thin Films Prepared By Spray Pyrolysis

M. A. Kaid

Physics Department, Minia University, El Minia, Egypt.

Email: makaied2000@yahoo.com

*Amorphous and crystalline vanadium pentoxide ( $V_2O_5$ ) thin films were grown onto heated glass substrates using spray pyrolysis technique. Aqueous solution of ammonium meta-vanadate with different concentrations ranging from 0.1 to 0.5M was used. X-ray diffraction study of  $c$ - $V_2O_5$  revealed polycrystalline films of orthorhombic structure with a preferred orientation (001). Voigt analysis of single reflection was used to determine crystallite size and microstrain. The refractive index  $n$  and the extinction coefficient  $k$  have been computed from the corrected transmittance and reflectance over the spectral range 300 to 2500 nm. Analysis of the absorption coefficient versus photon energy revealed allowed direct transitions with energy gap 2.34eV. The electrochromic behaviour has been investigated using three-electrode cell. Upon sodium insertion, the results showed that the changes in the optical absorption are consistent with the colour changes of the film. On applying the voltage the optical absorption in the wavelength range 500 – 900 nm increases and the absorption edge shifts towards lower energies. The film colouration showed to be stable over several tens of hours claiming high colouration memory. Due to its limited optical modulation,  $V_2O_5$  films may be useful as a passive counter electrode in conjunction with an active working electrode in complementary electrochromic devices.*

## 1. Introduction:

Due to the diverse structural, magnetic, electrical and optical properties of transition metal oxides, they found widespread applications in different fields like, optoelectronics, microelectronics, solid state ionics [1-3], microbatteries and electrochromic display devices [3,4]. Vanadium oxygen systems ( $V_2O_5$ ,  $VO_2$ ) have been studied intensively by theoretical and experimental techniques [3,5]. They show metal-semiconductor transition, which implies an abrupt change in optical and electrical properties [6]. That is why this oxide is used in thermal sensing and switching. Vanadium pentoxide

based materials are known to display several types of chromogenic effects [7], as a window for solar cells [8] and for transmittance modulation in smart windows with potential applications in architecture and automotives [9]. It shows an atypical behaviour because it can not be defined exactly either as a cathodically or as anodically coloring material.  $V_2O_5$  exhibit multi-colored electrochromism allowing the use in electrochromic (EC) displays color filters and other optical devices [1, 10]. The device performance is related to the structural properties and morphological features of the film, which in turn dependant on the deposition technique as well as the preparative parameters. Vanadium pentoxide films have been prepared using various physical and chemical techniques such as, thermal evaporation, electron beam evaporation, rf sputtering, dc magnetron sputtering, sol-gel, electrochemical deposition and pulsed laser ablation [10-21]. The first synthesis of polycrystalline  $V_2O_5$  and  $V_4O_9$  thin films prepared by spray pyrolysis technique has been reported [21]. Vanadium pentoxides of different crystallinity have been also prepared using sol-gel method [22].

However, it has been reported that the material stoichiometry is a major problem in the deposition of  $V_2O_5$  films and it is difficult to obtain [23]. Several studies have been carried out on the electrochromic properties of  $V_2O_5$  films prepared by spin coating [24, 25], vacuum evaporation [10], r.f. sputtering [14, 26], and sol gel [27].

In the present paper, vanadium pentoxide thin films have been prepared by spray pyrolysis using ammonium meta vanadat solution as precursor. The effect of substrate temperature and solution molarities on the structural as well as the optical properties is presented. The electrochromic behaviour of the prepared films have been studied using three-electrode cell. The influence of sodium intercalation on the optical absorption of the films is also presented.

## 2. Experimental Work:

Vanadium pentoxide thin films have been deposited from aqueous solution of ammonium meta-vanadate,  $[NH_4VO_3]$  in concentration range from 0.1 to 0.5M using spray pyrolysis technique. A home made spraying system has been developed to obtain high quality films. The solution was sprayed onto preheated glass as well as fluorine doped tin oxide glass substrates, kept at two different fixed temperatures, namely, 250°C and 400°C. The overall reaction process can be expressed as heat decomposition of ammonium meta-vanadate to form clusters of vanadium pentoxide in the presence of water. Prior to deposition, the substrates were chemically and ultrasonically cleaned. To avoid excessive cooling of the substrates, successive spraying process was used with

time period of 3 seconds between successive bursts. Compressed air at pressure of 5 N. cm<sup>-2</sup> has been used as a carrier gas; the solution flow was 6 cm<sup>-3</sup> min<sup>-1</sup>. In order to optimize the solution concentration, the substrate temperature, the nozzle to substrate height and deposition time were kept constant at, either 250°C or 400°C, 25cm, and 45s respectively. To ensure film homogeneity, the substrate was supported onto a rotating disc provided with a heater. The substrate temperature was controlled by a chrome-nickel thermocouple fed to a temperature controller. The film thickness was measured by multiple-beam Fizeau fringes at reflection using monochromatic light.

To investigate the structure of the film, a JEOL X-ray diffractometer (model JSDX-60PA) using Ni-filtered Cu K<sub>α</sub> radiation ( $\lambda_{\text{ka}} = 1.5148 \text{ \AA}$ ), was employed. Continuous scanning was applied with a slow scanning speed (10°/min) and a small time constant (1sec). A range of (2 $\theta$ ) from 10° to 70° was scanned, so that all possible diffraction peaks could be detected. The crystallite /size (CS) and the magnitude of micro-strain were determined using Voigt profile analysis. A parameter of interest with the Voigt function is “the shape parameter” defined as  $\phi = \text{FWHM}/\text{Integral breadth}$ . The value of this parameter is used to determine the fractional Lorentzian (Cuchy),  $\beta_{\text{L}}$ , and Gaussian  $\beta_{\text{G}}$  components in the convolute. The diffraction plane (001) was used for the evaluation of the micro-structure parameters. The obtained values are accurate within 4-5% as may account for the uncertainties in FWHM measurements. It is worth mentioning that the particle within a given sample are, of course, not of uniform size, therefore, one can speak only on an average crystal size within the sample.

In the solar spectral range, transmission and reflection measurements were carried out using Shimadzu UV 3101 PC; UV-VIS-NIR double beam spectrophotometer with reflection attachment of V-N type (incident angle 5°). A developed computer program [28] based on solving the exact equation was used to calculate the refractive index  $n$  and the extinction coefficient  $k$ . The prepared vanadium pentoxide films, deposited onto fluorine-doped tin oxide (FTO) coated glass substrates, were subjected to electrochemical ion insertion/extraction in an electrochemical solution containing 1M NaOH aqueous solution. A three-electrode cell has been used. Besides the working electrode (V<sub>2</sub>O<sub>5</sub> film), a platinum sheet has been used as a counter electrode. The reference electrode was a saturated calomel electrode (SCL).

### 3. Results and Discussion:

The as grown Vanadium pentoxide films have uniform yellow colour similar to those prepared by other techniques. Such yellow color could indicate that vanadium was incorporated as V<sup>+5</sup> in V<sub>2</sub>O<sub>5</sub> lattice, because, it is known that V<sup>+4</sup> presents a brown or black color [29]. However, it was shown that, films

prepared by thermal evaporation had light green tint that turned yellow upon annealing in  $O_2$  atmosphere at  $350^\circ C$  for 20 minutes, like  $V_2O_5$  starting powder [17].

Figure (1) shows the variation of film thickness, as determined interferometrically, versus solution molarities. It is clear that, as the solution molarity increases, the amount of material that participates in forming the deposited film increases with subsequent increase in the film thickness. Each data point is averaged from five measurements taken at different locations on the film, the calculated error was found to be  $\pm 7\%$ . This variation in film thickness is considered in the subsequent calculation.

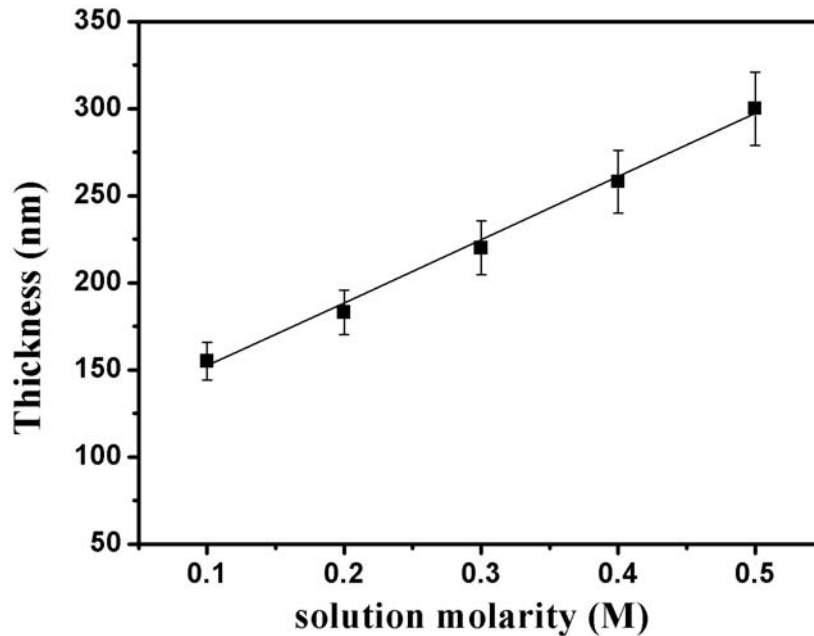
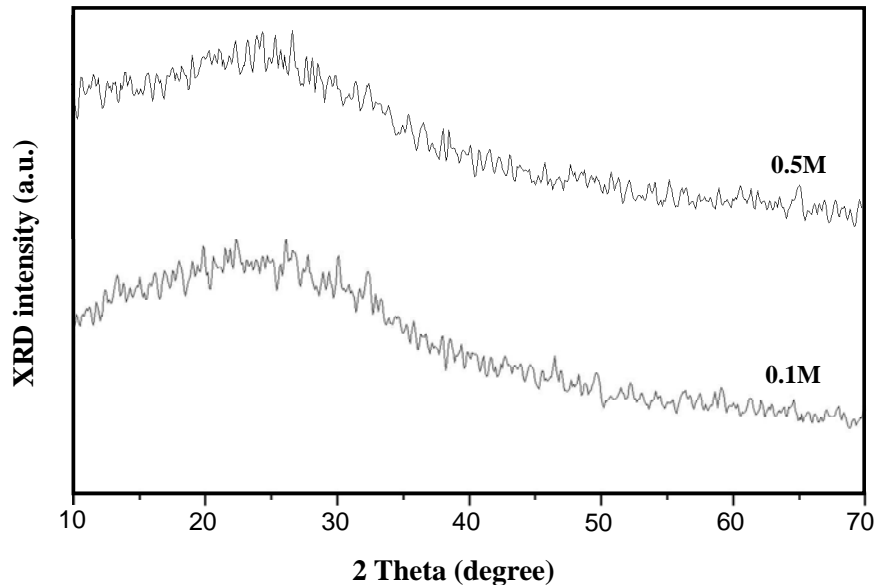


Fig. (1): Variation of thickness of sprayed  $V_2O_5$  thin films with solution molarity.

### 3.1. Structure

Figure (2) shows the diffraction pattern of vanadium pentoxide film deposited at substrate temperature  $T_s = 250^\circ C$  indicating that the structure is amorphous in nature characterized by a hump around  $2\theta = 25$  degrees. Films deposited at  $T_s = 400^\circ C$  shows crystalline structure characterized by three peaks at nearly  $2\theta = 20^\circ$ ,  $30^\circ$  and  $40^\circ$ . Published study showed that crystallization of  $V_2O_5$  films prepared onto amorphous glass substrates by physical deposition methods, starts in the temperature range  $300-500^\circ C$  [3, 30, 31]. However, using laser ablation, crystalline  $V_2O_5$  thin films were grown onto amorphous glass substrates at temperature as low as  $200^\circ C$  [32] due to the high kinetic energy of the ionized and ejected species [33]. By using vacuum evaporation technique

[34], amorphous and polycrystalline  $V_2O_5$  films with orthorhombic symmetry were obtained at substrate temperatures  $\leq 200^\circ\text{C}$  and  $\geq 300^\circ\text{C}$ , respectively. Also,  $V_2O_5$  and  $V_4O_9$  thin films were obtained on glass substrates by spraying a vanadium trichloride solution at substrate temperatures  $250^\circ\text{C}$  and  $200^\circ\text{C}$ , respectively [21].



**Fig. (2):** XRD patterns of  $V_2O_5$  thin films sprayed at  $T_{\text{sub}}=250^\circ\text{C}$  from different solution molarity.

The obtained XRD patterns at  $T_{\text{sub}}=400^\circ\text{C}$  (Fig.(3)), indicate the formation of polycrystalline vanadium pentoxide. The film crystallinity increases with increasing the solution molarity as manifested by the enhancement of the diffraction quality (peak-to-noise ratio). The peaks are indexed as orthorhombic  $V_2O_5$  (ICDD card# 09-0387). The peaks located at  $2\theta \approx 20^\circ$  and  $40^\circ$  degrees are attributed to the (001) and (002) lattice planes. The small peak located at  $2\theta \approx 30^\circ$  corresponds to  $V_4O_9$  phase whose intensity decreases with solution concentration and vanishes completely for films sprayed from solutions  $\geq 0.2\text{M}$ . Growth of the two phases have been also obtained by spraying vanadium nitrate onto glass substrate kept at two different temperatures, namely  $200$  and  $250^\circ\text{C}$  [18]. In a recent paper [35], crystalline vanadium pentoxide films ( $V_2O_5$ ) have been prepared by spraying vanadium nitrate of concentration  $\geq 0.1\text{M}$ , onto glass substrate kept at  $350^\circ\text{C}$ . In those experiments [18, 35], the preparative parameters are relatively lower than those used in the present work. Such differences are attributed to the different starting precursor which could be explained as follows:

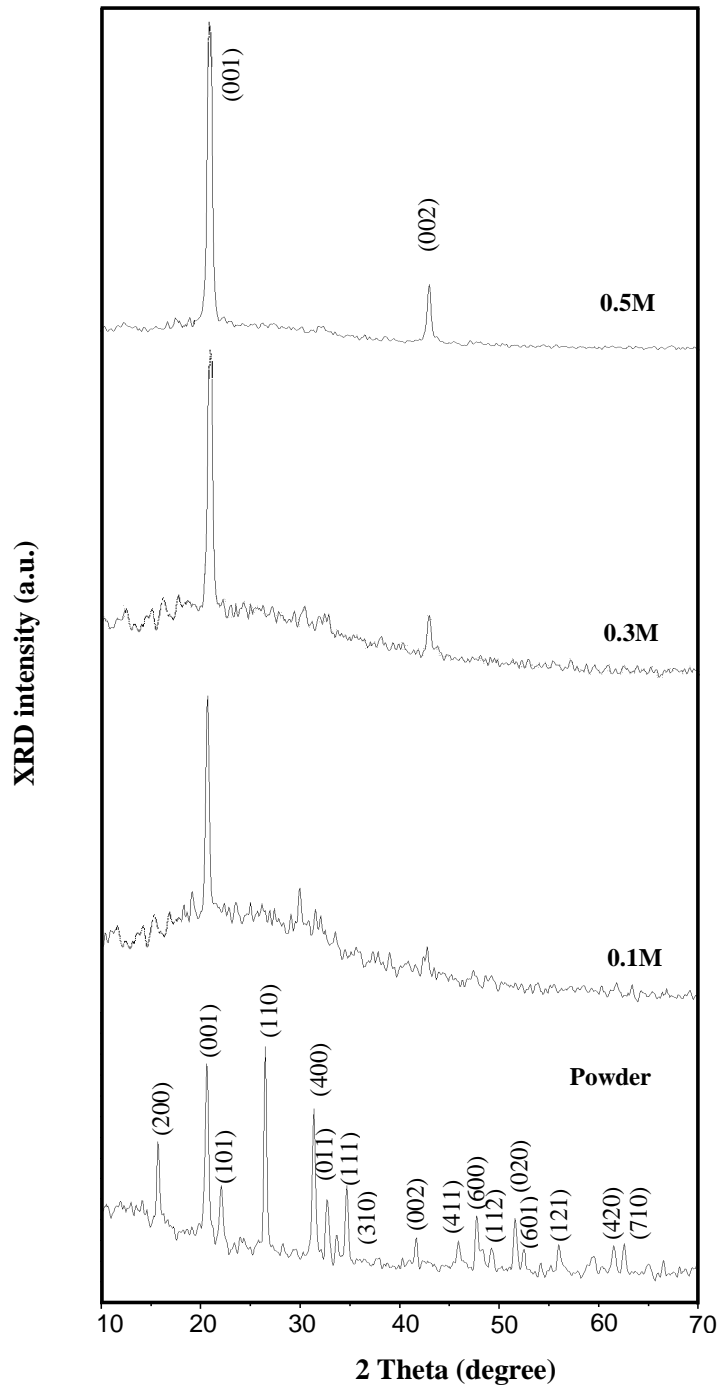
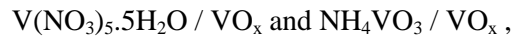


**Fig. (3):** XRD patterns of  $V_2O_5$  powder and thin films sparyed from different solution at  $T_{\text{sub}}= 400^\circ\text{C}$

The chemical composition of metal oxides thermally generated from inorganic precursor may be influenced by the type of chemical reactivity of volatile components of the precursor [36].

Considering the present precursor oxide systems, namely;



The solution chemistry of the precursor compounds involves ionization followed by aquation, as demonstrated by the following equations;

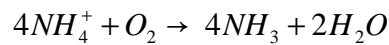


and,

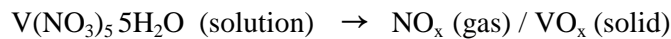


It is obvious from these ionization/aquation reactions that the former precursor compounds  $V(NO_3)_5 \cdot 5H_2O$  results in  $[V(H_2O)_n]^{+5}$  ionic species carrying a net positive charge (5+), whereas the latter compound  $NH_4VO_3$  leads to ionic species  $(VO_3)_{aq}^-$  acquiring a net negative charge (-1).

Upon drying and heating to the onset of thermal decomposition the companion anions  $(NO_3)^-$  of  $[V(H_2O)_n]^{+5}$  decompose releasing a mixture of  $NO_x$  gases furnishing an oxidizing atmosphere. In contrast, the companion cations  $(NH_4)_{aq}^+$  of  $(VO_3)_{aq}^-$  decompose releasing  $NH_3$  gas phase



which is a reducing atmosphere. Hence, the vanadium containing ionic species resulting from the two different precursors should establish the following different gas/solid interfaces;



Accordingly, the thermochemical interactions at the  $NO_x(g) / VO_x(s)$  would enhance the oxidation of  $VO_x$  leading to favourable conditions of  $V_2O_5$ . In contrast, the interactions at  $NH_3(g) / VO_x(s)$  would suppress the oxidation of  $VO_x$ , thus, retarding the formation of  $V_2O_5$ .

Since the (00h) peaks were observed, only the c-axis was calculated. The lattice parameters calculated from Fig.(3) and those found in literatures are summarized in Table (1), showing good coincidence for the c-axis.

Table (1): Lattice parameter (c-axis).

Reference	c (Å)
Present work	4.373
[21]	4.380
[37]	4.369
[38]	4.368
[39]	4.430

From Fig. (3), it is clear that, the solution molarity in the range 0.1- 0.5M and at  $T_s = 400^\circ\text{C}$  lead to the formation of well crystallized vanadium pentoxide strongly oriented along the (001) plane. Intensities of (001) reflection are given in Table (2) for different molarities and the results reveal the increase of film ordering with increasing molarity. The dominance of the (001) peaks in the XRD pattern suggests that the spray deposited  $\text{V}_2\text{O}_5$  thin films are oriented with the c-axis perpendicular to the surface of the substrate. Similar findings were obtained for  $\text{V}_2\text{O}_5$  films sputtered onto corning glass [18, 29] and ITO substrates [40]. Also,  $\text{V}_2\text{O}_5$  film grown by pulsed laser deposition (PLD) deposited at  $T_s = 200^\circ\text{C}$  in oxygen partial pressure of 100 mTorr exhibit the predominant (001) peak of orthorhombic  $\text{V}_2\text{O}_5$  phase [31]. Using dc sputtering technique, it was reported that, whatever the oxygen low, the use of a dc power of 100 W leads to the formation of well crystallized  $\text{V}_2\text{O}_5$  films strongly oriented with the ab planes parallel to the substrate showing a (001) preferred orientation[39]. Films prepared by rf sputtering, onto different substrates, showed orthorhombic structure having a c-axis preferred growth orientation[41]. The preferred orientation is related to the in plane organization of the V-O-V chains. The layer-like structure of  $\text{V}_2\text{O}_5$  is built up from distorted trigonal bipyramidal coordinated polyhedra of oxygen atoms around vanadium atoms, which share edges to form  $(\text{V}_2\text{O}_4)_n$  zig-zag double chains along the  $\langle 001 \rangle$  direction and are cross-linked the (002) plane through shared corners and thus forming sheets in the x-y plane [42].

The microstructure parameters, crystallite size and micro-strain of the prepared vanadium pentoxide films have been determined using profile analysis of (001) plane. The calculated crystallite size and micro-strain and their variations with solution molarities are given in Figs.(4) and (5), respectively. The depicted values are accurate within  $\pm 6\%$  according to the uncertainties associated with profile half-width measurements. Films prepared with solution molarity 0.1M is composed of particles with an average size of 24nm which

increases with solution concentration reaching 40nm at 0.4M. Smaller values of 17 nm were obtained for films thermally evaporated at  $T_s = 300^\circ\text{C}$  [34]. Larger value, 60nm, have been grown at  $T_s = 350^\circ\text{C}$  using spray pyrolysis. Differences in crystallite size may be attributed to the difference in the used precursor and the set-up parameters adopted in the experiments. The crystallite size is, by definition, measured in direction normal to the reflecting plane, i.e. in  $\langle 001 \rangle$  direction, and consequently perpendicular to the substrate. Therefore, any increase in the crystallite size may be attributed in terms of a columnar grain growth associated with growing of film thickness.

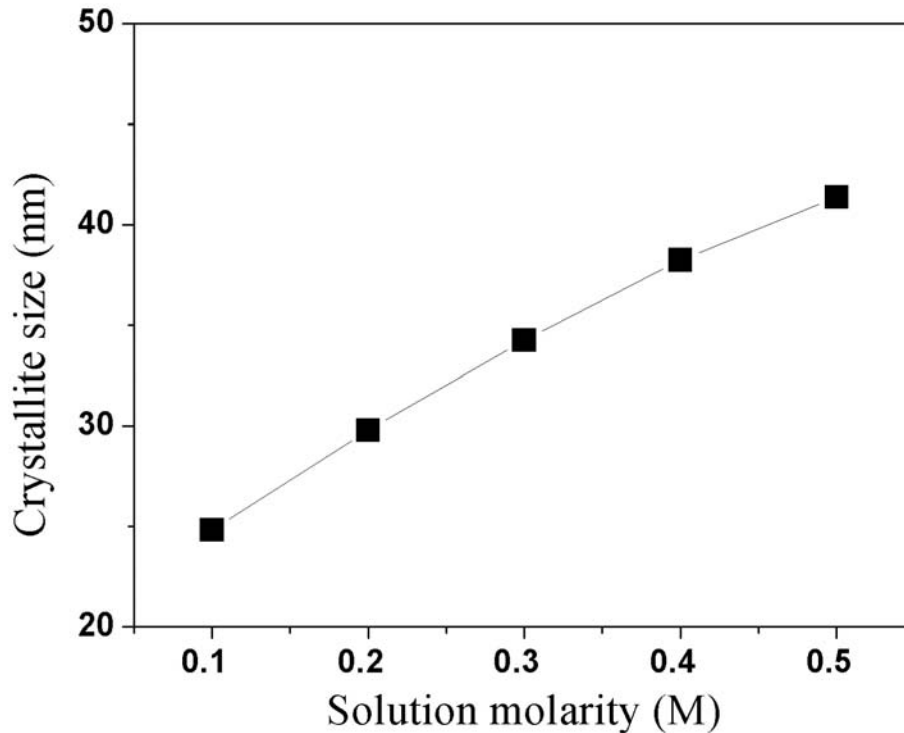


Fig. (4): The variation of grain size of  $\text{V}_2\text{O}_5$  thin films versus solution molarities.

The calculated microstrain of the investigated samples changes from  $4.53 \times 10^{-3}$  to  $10.72 \times 10^{-3}$  as the solution molarities increases from 0.1 to 0.5 M. Comparable values of  $3.132 \times 10^{-3}$  and  $4.387 \times 10^{-3}$  reported for thermally evaporated films [34]. The observed increase in film strain shown in Fig.(5), may be related to the temperature miss-match between the formed underlayer and the newly sprayed solution accompanied with film relaxation due to water release. This phenomenon is exaggerated at larger film thickness deposited from higher solution concentration (0.5M).

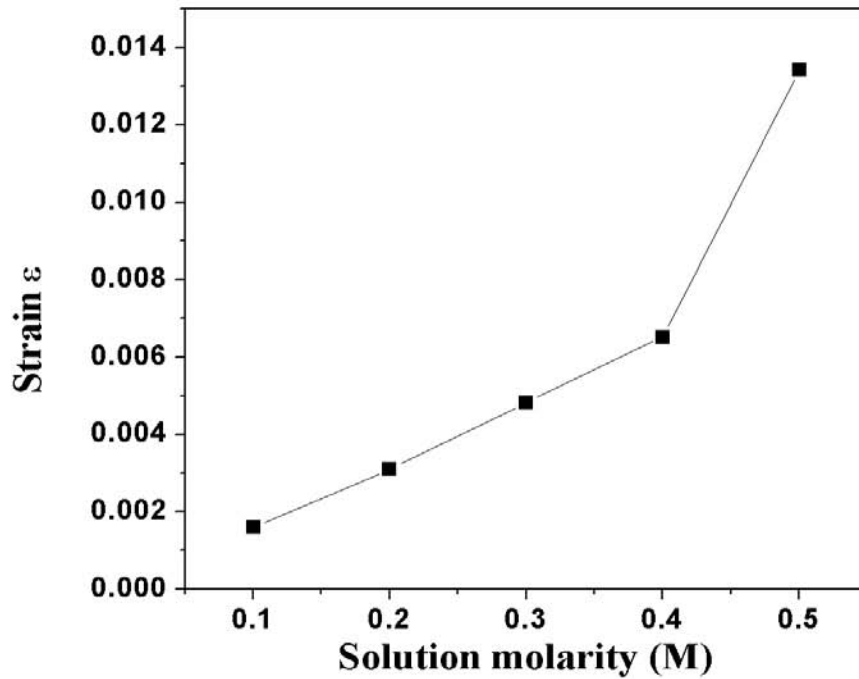


Fig. (5): The variation of strain ( $\epsilon$ ) of  $V_2O_5$  thin films with solution molarities.

### 3.2. Optical Properties:

The spectral transmittance and reflectance, measured in the range 300-2500nm, of vanadium pentoxide films sprayed onto glass substrates kept at  $T_s = 400^\circ\text{C}$  are shown in Fig. (6). The results indicate that the transmission over the whole spectral range investigated, is lowered with increasing solution concentration. This is due to the higher film absorption associated with larger film thickness. Films prepared with concentration 0.1M, show higher transmission exceeding 80% over the whole spectral range investigated, with a well defined absorption edge lying in the UV region. For higher molarities, 0.2-0.5M, besides the reduction in intensity, shifts in the transmission threshold to lower energy is observed. Similar observations have been found for films sprayed at  $200^\circ\text{C}$  from vanadium trichloride solutions of different molarities and reported recently [35]. The reflectance spectra for the same films showed similar trends as transmittance curves, films prepared from higher solution concentrations shows lower reflectance, However, beyond the absorption edge, the summation of  $T(\lambda) + R(\lambda)$  does not equal to one, indicating presence of either light scattering, absorption or both. This is consistency with the visual appearance of the films surfaces particularly for larger thickness. Therefore, for subsequent computation of optical constants, the reflectance values were

corrected for the diffused component as measured by the integrating sphere provided by the used spectrophotometer. Moreover, results of film thickness measurement given in Fig.(1), indicate that films prepared with solution concentration 0.1M drops to one third its value at 0.5M due to less material participate in film growing. Therefore, the film thickness is another cause added to the effect of surface roughness, which participates in the drastic enhancement of film transmission for films prepared with lowest solution concentration.

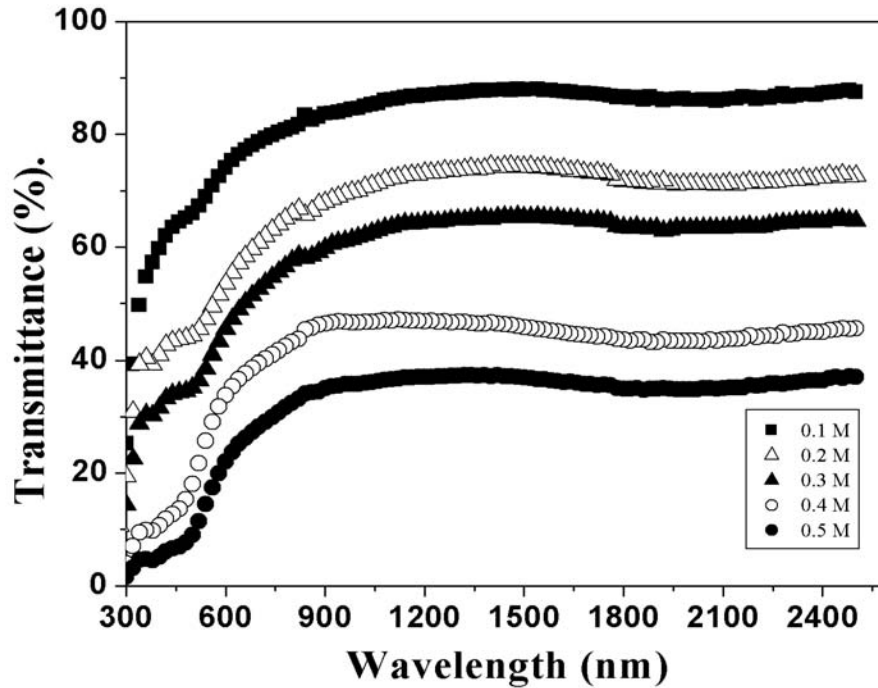


Fig. (6): Spectra transmittance of sprayed  $V_2O_5$  films of different solution molarities,  $T_{sub} = 400\text{ }^\circ\text{C}$ .

For determination of the optical constants we have used the spectrophotometric data corresponding to films prepared with  $>0.2\text{ M}$  solution giving stoichiometric and transparent films. The optical constants, the refractive index  $n$  and the extinction coefficient  $k$ , of the prepared films have been computed from the measured and corrected transmittance and reflectance values over the investigated range. A home developed computer program [28] based on solving Murmann's exact equations [43] has been used. The method involves a bi-variant search technique based on minimizing  $(\Delta R)^2$  and  $(\Delta T)^2$  simultaneously, where  $(\Delta R)^2 = R_{exp} - R_{cal}$  and  $(\Delta T)^2 = T_{exp} - T_{cal}$ . In this work, Tomlin function [17] namely,  $(1 + R)/T$  and  $(1 + T)/R$  were used as two simultaneous variables instead of  $R$  and  $T$ . The spectral behaviour of the

calculated refractive index,  $n$ , for films deposited with solution molarity 0.1M, is shown in Fig.(7)-a. It shows abnormal dispersion in the wavelength range lower than the absorption edge and posses a peak at  $\lambda = 450$  nm after which  $n$  decreases with wavelength showing normal dispersion. The refractive index values drops from 2.6 at  $\lambda = 400$  nm to 1.8 at  $\lambda = 2400$  nm. Similar values and behaviour have been reported recently for vanadium pentoxide mixed with cerium oxide [43]. At long wavelengths, the  $n$  values are nearly 1.8. This is to be compared with the reported values of 1.8, 1.9, 2.12 and 2.18 for films prepared with sprayed vanadium nitrate, evaporation from Mo boat, e-beam evaporation and sputtering, respectively [35, 45, 31].

The obtained values depicted in Fig.(7)-a are averaged of five calculated results and fitted by Sellmeir's relation:

$$n = n_{\infty} + [b/\lambda^2 - \lambda_0^2]$$

where "b" and " $\lambda_0$ " are constants and " $n_{\infty}$ " represents the refractive index far from the absorption edge. The best fit, solid line, Fig.(7-a), yielded  $b = 210000$  (nm)<sup>2</sup>,  $\lambda_0 = .0119$ nm and  $n_{\infty} = 1.74$ . The calculated percentage error was found to vary between 3 at  $\lambda = 2500$  nm and 6 at  $\lambda = 300$  nm. Such error is acceptable with the computation method based on Murmann's exact equation used in this work. Such errors are mainly attributed to the experimental errors associated with the measured film thickness as well as spectrophotometric transmittance and reflectance measurements.

The absorption coefficient  $\alpha$  has been calculated by the relation  $\alpha = 4\pi k/\lambda$ , where  $k$  is the computed extinction coefficient, then depicted in Fig.(7)-b. It shows that  $\alpha$  varies slightly in the wavelength range from 900 to 2500 nm causing an absorption tail which may attributed to either amorphous material in the film or film off-stoichiometry or both. Again, absorption for wavelengths lower than 900 nm is attributed to the presence of  $V^{4+}$  ions and depends on their density [43].

For absorption curves, characterized by an Urbach edge, one can estimate the width of the band tail by the relation [46]:

$$\alpha = \alpha_0 \exp (hv/E_0)$$

where  $\alpha_0$  is a constant and  $E_0$  is the band tail width. The value of  $E_0$  has been estimated from the slope of  $\ln\alpha$  versus  $h\nu$  plot. This has been done for films prepared at different molarities. The obtained results, given in Table (2), shows that the band tail width,  $E_0$  increases with decreasing solution molarity. Such findings are consistent with the appeared tails in the spectral transmittance curves obtained at different molarities, Fig.(6).

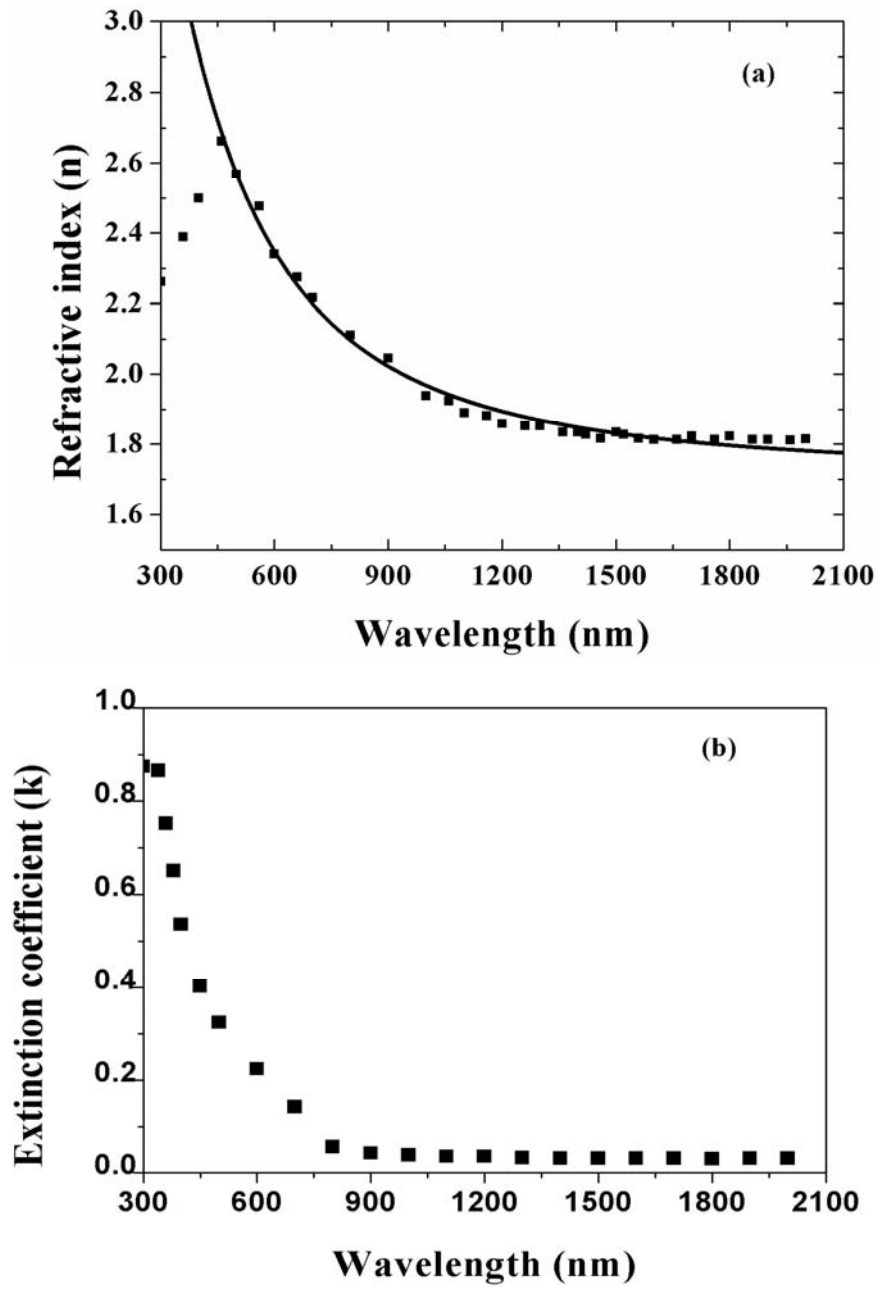


Fig. (7): Spectral variation of: a) refractive index (n) and b) extinction coefficient (k) of V<sub>2</sub>O<sub>5</sub> thin film.

Table (2): Intensities of (001) reflection and band tail width.

Concentration (M)	Intensity (a. u.)	Band tail, $E_o$ (eV)
0.1	19.1	2.250
0.2	26.2	0.581
0.3	35.0	0.514
0.4	44.5	0.459
0.5	96.0	0.399

At incident photon energy higher than that region mentioned above, the absorption coefficient steeply increases defining the absorption edge. The fundamental absorption edge of semiconductors corresponds to the threshold for charge transitions between the highest nearly filled band and the lowest nearly empty band. The absorption is very small for photon energies much less than the energy gap and increases significantly for higher photon energies.

The inter-band absorption theory shows that, the absorption coefficient near the threshold versus incident energy, is given by the relation [47],

$$(h\nu\alpha) = A_n [h\nu - E_g]^n \quad (1)$$

where  $A_n$  is the probability parameter for the transition,  $E_g$  is the optical band gap and  $n$  is an index determined by the nature of the electron transition during the absorption process. The present results were found to obey Eqn.(1) with  $n = (1/2)$  indicating allowed direct transition. The direct band gap energy is given by the intersection of the resulted straight line and the horizontal axis on plots of  $(\alpha h\nu)^2$  vs. the incident photon energy  $h\nu$  then depicted in Fig.(8). The results revealed  $E_g^d = 2.34$  eV, which is comparable with the value 2.2 eV and from 2.2 to 2.3eV for the sputtered films reported in [40,44] and [24,31,48], respectively. Lower values 1.90-2.18 eV were calculated for films prepared by different methods [14, 49, 50]. Relatively higher values, 2.24-2.5 eV, were reported for films of different thickness prepared by r.f. reactive sputtering [41]. Different findings have been recently reported for films deposited onto glass substrates at 200°C by spray pyrolysis [51]. They obtained a direct band gap,  $E_g^d = 2.44$  eV, which is in agreement, as they reported, with previous results. Table (3) gives the obtained optical energy gap value and the type of transition in comparison with the most recent published results. It shows that the type of transition is mostly allowed direct one as revealed in the present work, while noticeable differences are found in the energy gap values. Such differences could be attributed to the different methods of preparation. In addition, substrate temperature and starting precursor which affect, not only the film stoichiometry, but also the degree of crystallinity, since more ordering leads to decrease of the localized states in the band gap which causes lowering of the energy gap.

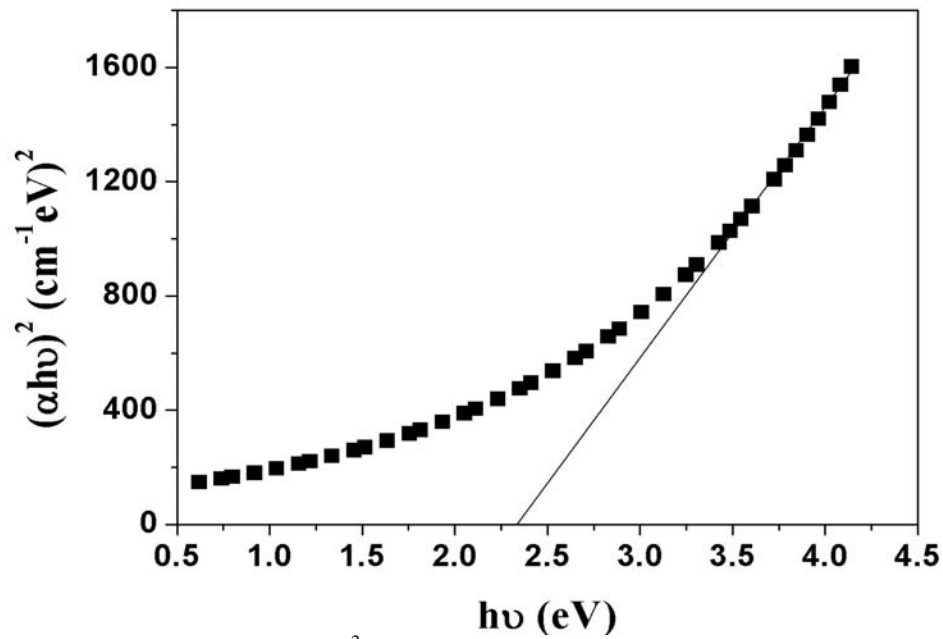


Fig. (8): Plot of  $(\alpha h\nu)^2$  versus photon energy ( $h\nu$ ) for  $V_2O_5$  thin film.

Table (3): Value and type of the optical energy gap.

Ref.	Method of preparation	Structure	$E_g$ Direct (eV)	$E_g$ Indirect (eV)
[29]	Sol-gel method	Orthorhombic	2.49 as deposited 2.42 annealed	-----
[47]	r.f. sputtering	Orthorhombic	-----	2.2-2.3
[28]	Spray pyrolysis $T_s=250^\circ\text{C}$	Orthorhombic	2.44	-----
[55]	r.f. Sputtering	Orthorhombic	2.24 - 2.50	-----
[23]	Vacuum evaporation	Orthorhombic	2.03	-----
[41]	Spray pyrolysis $T_s=350^\circ\text{C}$	Orthorhombic	2.50	2.33
Present work	Spray pyrolysis $T_s=400^\circ\text{C}$	Orthorhombic	2.34	-----

### 3.3. Electrochromic:

Figure.(9) shows the spectral transmittance of  $V_2O_5$  film deposited onto FTO glass substrate kept at  $400^\circ\text{C}$  and with solution concentration of 0.2M. The film has been colored at different coloration potentials namely, -1, -2 and -4 volts and bleached at +4 volts. The results depicted in Fig.(9) shows that, by elevating the coloration potential, the film transmittance decreases due to the increase of film absorption over the wavelength range 600 – 1800 nm. At = 950, which defines the transmittance peak, it is lowered by nearly 50%. This is to be compared with 20% reported by sputtered films in the modulation range 600 – 900 nm [14]. Such relatively higher optical modulation value, obtained in this work and those previously reported, lead to conclusion that vanadium pentoxide films may be useful as a passive counter electrode in conjunction with an active working electrode in complementary electrochromic devices.

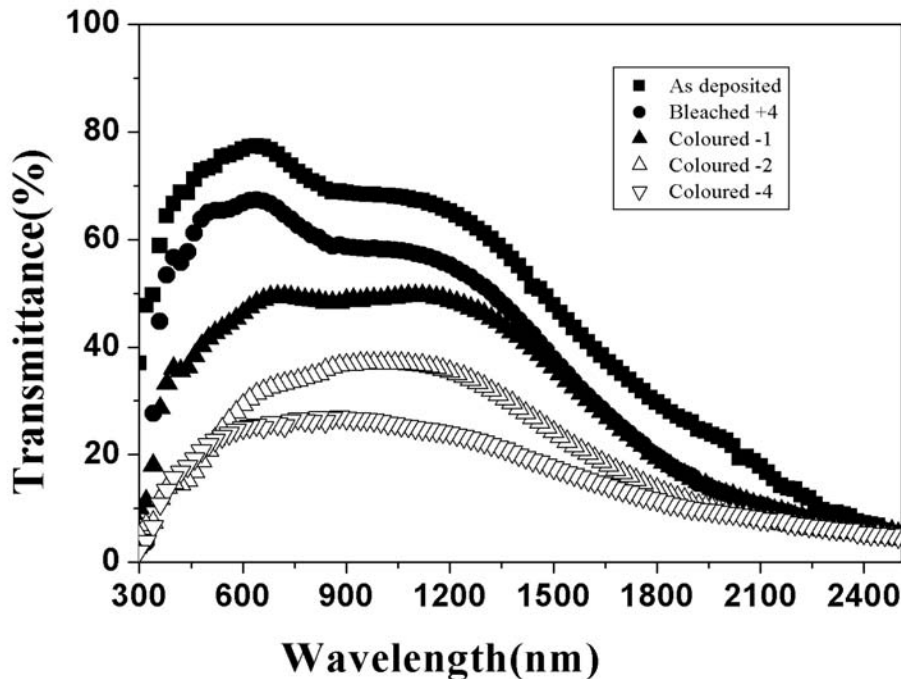


Fig. (9): Spectral optical transmittance versus wavelength of  $V_2O_5$  thin film.

#### 4. Conclusion:

Films sprayed from ammonium meta-vanadate of different concentration and at temperatures  $T_s = 250^\circ\text{C}$  are amorphous, while films deposited at  $T_s = 400^\circ\text{C}$  showed to be polycrystalline with orthorhombic symmetry having a c-axis preferred growth orientation. Single phase  $\text{V}_2\text{O}_5$  is formed from concentrations  $\geq 0.2\text{M}$ . With the lowest concentration (0.1M), beside the formation of  $\text{V}_2\text{O}_5$ , a  $\text{V}_4\text{O}_9$  appeared was identified. Increasing the solution concentration increases the crystallite size from 24 to 40 nm and the strain from  $1.5 \times 10^{-3}$  to  $13 \times 10^{-3}$ . The increase in film strain may be related to the temperature mismatch between the formed underlayer and the newly sprayed solution accompanied with film relaxation due to water release. The spectral variation of refractive index, showed anomalous dispersion in the blue region followed by normal variation obeying Sellmeier relation. Analysis of the absorption curves revealed allowed direct transition with optical energy gap 2.34eV. Electrochromic investigation showed that, the changes in the films colouration are consistent with the optical absorption in the wavelength range 500-900nm. Also, the absorption edge shifts towards lower energies. The film colouration showed to be stable over several tens of hours claiming high colouration memory. Due to its limited optical modulation,  $\text{V}_2\text{O}_5$  films may be useful as a passive counter electrode in conjunction with an active working electrode in complementary electrochromic devices.

#### References

1. S.F. Cogan, N.M. Nguyen, S.T. Perrotti, R.D. Rauh, *Proc. Soc. Photo-Opt. Instrum. Eng.* **57**, 1016 (1988).
2. C.G. Granqvist, *Solid State Ionics* **70**, 678 (1994).
3. C.M. Julien, *Ionics* **2**, 169 (1996).
4. M.E. Spahr, P.S. Bitterli, R. Nesper, O. Haas, P. Novak, *J. Electrochem. Soc.* **146**, 2780 (1999).
5. E.A. Meulenkamp, W. van Klinken, A.R. Schlattmann, *Solid State Ionics* **126**, 235 (1999).
6. J. Haber, M. Witko, R. Tokarz, *Appl. Catalysis A General* **157**, 3 (1997).
7. C.M. Lampert, C.G. Granqvist, editors, large Area Chromogenic materials and Devices For Transmittance Control, Bellingham: SPIE, (1990).
8. S.D. Hansen, C.R. Aita, *J. Vac. Sci. Technol.* **A3**, 660 (1985).
9. MSR. Khan, K.A. Khan, W. Estrada, C.G. Granqvist, *J. Appl. Phys.* **5**, 69 (1991).
10. Y. Fujita, K. Miyazaki, T. Tatsuyama, *Jap. J. Appl. Phys.* **24**, 1082 (1985).
11. J.B. Bates, N.J. Dudney, G.R. Robertson, *J. Power sources* **43**, 103 (1993).
12. A.Z. Moshfegh, A. Ignatiev, *Thin Solid Films* **198**, 253 (1991).

13. M.N. Field, I.P. Parkin, *J. Mater. Chem.* **10**, 1863 (2000).
14. [14]M. Benmoussa, A. Outzourhit, A. Bennouna, E.L. Ameziane, *Thin Solid Films* **405**, 11 (2002).
15. T.J. Hanlon R. E. Walker, J.A. Coath, M. A. Richrdson, *Thin Solid films* **405**, 234 (2002).
16. M. Losurdo D. Barreca, G. Bruno, E. Tondello, *Thin Solid films* **384**, 58 (2001).
17. Guangming Wu, Kaifang Du, Changsheng Xia, Xiao Kun, Jun Shen, Bin Zhou, Jue Wang, *Thin Solid films* **485**, 284 (2005).
18. M. Benmoussa, E. Ibnouelghazi, A. Bennouna, E.L. Ameziane, *Thin Solid Films* **265**, 22 (1995).
19. M.G. Krishna, Y. Debaugé, A.K. Bhattacharya, *Thin Solid Films* **312**, 116 (1998).
20. C. Julien, E. Haro-Poniatowski, M.A. Camacho-Lopez, L. Escobar-Alarcon, *J. Jimenez-Jarquín, Mater. Sci. Eng.* **B65**, 170 (1999).
21. A. Bouzidi, N. Benramdane, A. Nakrela, C Mathieu, B. Khelifa, R. Desfeux, A. Da Costa, *Mater. Sci. Eng.* **B95**, 141 (2002).
22. Z.S. ElMandouh, M.S. Selim, *Thin solid films* **371**, 259 (2000)
23. K.M. Park, S. Yi, S. Moon, S. Im, *Optical Materials* **17**, 311 (2001).
24. Y. Shimizu, K. Nagase, N. Miura, N. Yamazoe, *Jap. J. Appl. Phys.* **29**, L1708 (1990).
25. N. Nagase, Y. Shimizu, N. Miura, N. Yamazoe, *Appl. Phys. lett.* **60**, 802 (1992).
26. S.F. Cogan, N.M. Nguyen, S.T. Perrotti, R.D. Rauph, *J. Appl. Phys.* **66**, 1333 (1989).
27. J.P. Pereira-Ramos, R. Baddour, S. Bach, N. Baffer, *Solid Stat ionics* **53/56**, 701 (1992).
28. N. Elkadry, A. Ashour, M.F. Ahmed, K. Abdel-Hady, *Thin Solid Films* **229**, 194 (1995).
29. K. Melghit, S. P. Pillai, V. G. Kumar Das, *J. Mater. Sci. lett.* **18**, 661 (1999).
30. J.P. Audiere, A. Madi, I.C. Grenet, *J. Mater. Sci.* **17**, 2973 (1982).
31. C. V. Ramana, O. M. Hussain, B. Srinivasula Naida, P.J. Red, *Thin Solid Films* **305**, 219 (1997).
32. M. Benmoussa, E. Ibnouelghazi, A. Bennouna, Y. Laziz, E.I. Ameziane, *Le vide* **275**, 24 (1995).
33. D.G. Chrisey, G.K. Hubler (Eds), *Pulsed Laser Deposition of Thin Films*, Wiley, new York, (1994).
34. R.T. Rajendra Kumar, B. Karunagaran, V. Senthil Kumar, Y.L. Jeyachandran, D. Mangalaraj, Sa.K. Narayandass, *Materials science in Semiconductor processing* **6**, 543 (2003).

35. A.A.Akl, *Applied surface science* **252**, 8745 (2006).
36. M.I. Zaki, A.K.H. Nohman, C. Kappenstein and T. Wahdan, *Journal of Materials Chemistry*, **5**, 1081 (1995).
37. R. Enjalbert, J. Galy, *Acta Cryst.* **C42**, 1467 (1986).
38. C. Mathieu, S. Peralta, A. Da Costa, Y. Barbaux, *Surf. Sci.* **395**, 1201 (1998).
39. C. Navone, J.P. Preira\_Ramos, R. Baddour\_Hadjean, R. Salot, *J. Power Sources* **146**, 327 (2005).
40. M. Benmoussa, A. Outzourhit, A. Bennouna, E.I. Ameziane, *Thin Solid Films* **405**, 11 (2002).
41. L.Ottaviano, A. Pennisi, F. Simone, A.M. Salvi, *Optical Materials* **27**, 307-313 (2004).
42. L. Abello, E. Husson, Y. Repelin. G. Lucazeau, *Spectrochim. Acta* **39A**, 641 (1963).
43. O.S. Heavens, *Optical Properties of Thin Films*, Dover, New York, (1965).
44. E. Masetti, F. Varsano, F. Decker, A. Krasilnikova, *Electrochimica Acta* **46**, 2085(2001)
45. M.F.Al.Kuhaili, E.E.Khawaja,D.C.Ingram, S.M.A. Durrani, *J. Thin Solid Films* **460**, 30 (2004)
46. F. Urbach, *Phys. Rev.* **92**, 1324 (1953).
47. P.Kireev, *la physique des semiconductors*, Mir ed. Moscou, (1975).
48. R.D. Rauh, S.F. Cogan, *Solid State Ionics* **28-30** (1988).
49. C.R. Aita, Y-L Liu, M.L Kao, S.D. Hansen, *J. Appl. Phys.* **62**, 749 (1986).
50. J.C. ParkerD.I. Lam, Y.N. Xu, W.Y. Ching, *Phys. Rev. B* **42**, 5289 (1990).
51. A.Bouzidi, N.Benramdane, A.NaKrela, C.Mathieu, B.Khlifa, R.Desfeux, A.Da Costa, *Materials Science and Engineering* **B95**, 141 (2002).